Cellular Oncology 27 (2005) 225–230
IOS Press

Implementation of accurate and fast DNA cytometry by confocal microscopy in 3D

Lennert S. Ploeger [a], André Huisman [a], Jurryt van der Gugten [a], Dionne M. van der Giezen [a], Jeroen A.M. Beliën [b], Abdelhadi Y. Abbaker [b], Hub F.J. Dullens [a], William Grizzle [c], Neal M. Poulin [a], Gerrit A. Meijer [b] and Paul J. van Diest [a,*,**]

[a] *Department of Pathology, University Medical Center Utrecht, Utrecht, The Netherlands*
[b] *Department of Pathology, VU University Medical Center, Amsterdam, The Netherlands*
[c] *Department of Pathology, University of Alabama at Birmingham, Birmingham, AL, USA*

Abstract. *Background*: DNA cytometry is a powerful method for measuring genomic instability. Standard approaches that measure DNA content of isolated cells may induce selection bias and do not allow interpretation of genomic instability in the context of the tissue. Confocal Laser Scanning Microscopy (CLSM) provides the opportunity to perform 3D DNA content measurements on intact cells in thick histological sections. Because the technique is technically challenging and time consuming, only a small number of usually manually selected nuclei were analyzed in different studies, not allowing wide clinical evaluation. The aim of this study was to describe the conditions for accurate and fast 3D CLSM cytometry with a minimum of user interaction to arrive at sufficient throughput for pilot clinical applications. *Methods*: Nuclear DNA was stained in 14 μm thick tissue sections of normal liver and adrenal stained with either YOYO-1 iodide or TO-PRO-3 iodide. Different pre-treatment strategies were evaluated: boiling in citrate buffer (pH 6.0) followed by RNase application for 1 or 18 hours, or hydrolysis. The image stacks obtained with CLSM at microscope magnifications of $\times$40 or $\times$100 were analyzed off-line using in-house developed software for semi-automated 3D fluorescence quantitation. To avoid sectioned nuclei, the top and bottom of the stacks were identified from ZX and YZ projections. As a measure of histogram quality, the coefficient of variation (CV) of the diploid peak was assessed. *Results*: The lowest CV (10.3%) was achieved with a protocol without boiling, with 1 hour RNase treatment and TO-PRO-3 iodide staining, and a final image recording at $\times$60 or $\times$100 magnifications. A sample size of 300 nuclei was generally achievable. By filtering the set of automatically segmented nuclei based on volume, size and shape, followed by interactive removal of the few remaining faulty objects, a single measurement was completely analyzed in approximately 3 hours. *Conclusions*: The described methodology allows to obtain a largely unbiased sample of nuclei in thick tissue sections using 3D DNA cytometry by confocal laser scanning microscopy within an acceptable time frame for pilot clinical applications, and with a CV small enough to resolve smaller near diploid stemlines. This provides a suitable method for 3D DNA ploidy assessment of selected rare cells based on morphologic characteristics and of clinical samples that are too small to prepare adequate cell suspensions.

Keywords: Confocal laser scanning microscopy, 3D, DNA ploidy, image analysis

1. Introduction

The DNA content of prostate cancer cells is strongly related to tumor grade and stage [1,5]. Confocal Laser Scanning Microscopy (CLSM) presents the opportunity to perform 3D DNA content measurements on intact cells in thick histological sections [13]. This has major advantages over the established techniques of flow cytometry and conventional 2D image cytometry on cytospins. The advantage is that dissociation of tissue with consequently loss of tissue architecture is not required, and inaccuracies caused by cutting or overlap as present in conventional image cytometry on thin tissue sections is almost completely avoided [7,14]. Since the content measurements on the nuclei are directly related to the images they are obtained from, other quantities can also be measured on those nuclei, which can together be used for classification purposes [10]. Furthermore, 3D DNA measurements are also possible on biopsy material of prostate tissue, where the amount of tissue is limited. However, to obtain a sample of nuclei

*Corresponding author: Paul J. van Diest, MD, PhD, Professor of Pathology, Department of Pathology, University Medical Center Utrecht, PO Box 85500, 3508 GA Utrecht, The Netherlands. Tel.: +31 30 2506565; Fax: +31 30 2544990; E-mail: p.j.vandiest@azu.nl.

**Supported by grant #1 R01-AG021397-01 of the NIH.

that is representative for the specimen remains a problem [6,11]. Typically, image stacks of optically sliced thick sections are acquired interactively, after which individual nuclei are manually segmented. Of these two steps image acquisition is relatively quick, although it may be more time consuming when several image stacks need to be combined to obtain a representative sample size. The manual segmentation procedure is traditionally very time consuming as it has been estimated that samples sizes of approximately 300 nuclei are necessary to arrive at a coefficient of variation (CV) of about 10% which allows resolution of smaller near diploid stemlines [6]. We previously described the first steps in automation of this technology by introducing automated collection of 3D image stacks and segmentation of nuclei [2]. However, the quality of the resulting histograms was yet insufficient for clinical application that requires detection of small aneuploid stemlines. At the same time, an even higher degree of automation was required to arrive at specimen throughput allowing initial clinical studies.

The aim of this study was therefore to develop a method for accurate and fast 3D CLSM based DNA cytometry suitable for pilot clinical studies. For this purpose, analysis of the image stacks was optimized by introduction of filtering of the automatically segmented objects to remove faulty objects and sectioned nuclei. The parameters involved to automatically segment the nuclei were set in such a way that user intervention was minimal. Further, the influence of several tissue processing steps on histogram quality was investigated to arrive at the optimal protocol.

2. Materials and methods

2.1. Tissue preparation

Healthy liver and adrenal tissue with the lowest CV as determined by DNA flow or image cytometry were selected. Tissue sections of 14 μm healthy paraffin-embedded tissue were cut. Several staining conditions were varied: incubation time of RNase A (1 or 18 hours), pretreatment with citrate buffer and hydrolysis, and DNA staining with either YOYO-1 iodide (488 nm excitation, maximum emission at 509 nm) or TO-PRO-3 iodide (633 nm excitation, maximum emission at 661 nm).

The first experiment compared liver and adrenal tissue staining with YOYO-1 and TO-PRO-3 (Molecular Probes, Eugene, OR, USA) for 2 hours at room temperature at a magnification of $\times$100 without additional zoom, applying no pretreatment. After rinsing with distilled water the tissues were mounted in Vectashield (Vector Laboratories, Burlingame, CA, USA) and sealed with a coverslip.

Having identified the normal tissue and stain providing the lowest CVs in the first experiment, for the second experiment, the duration of RNase A (Boehringer, Mannheim) treatment was varied (1 *versus* 18 hours). Magnification was again $\times$100.

Having identified optimal duration of RNase treatment in the second experiment, in the final experiment tissue sections were boiled for 20 min in a 10 mM sodium citrate buffer (pH 6.0) or hydrolyzed with 2 N HCl for 30 minutes at room temperature. Imaging was performed at magnifications of $\times$60 ($\times$40 objective combined with a zoom factor of 1.5) and $\times$100 ($\times$100 objective without additional zoom).

2.2. Image acquisition and analysis

Image stacks were acquired with a confocal laser scanning microscope (Leica TCS SP2 AOBS, Leica Microsystems, Heidelberg, Germany) fitted with $\times$40/1.25 NA and $\times$100/1.40 NA oil immersion objectives. With zoom factors of 1.5 and 1, respectively, final magnifications were achieved of $\times$60 and $\times$100. Zooming in our confocal system is achieved by adjusting the mirror settings leading to an increase in resolution. In each field of vision, stacks of approximately 100 2D digital images (512 $\times$ 512 pixels) were obtained, depending on the effective thickness of the tissue sections. The bottom and top of the stack were identified interactively as the slices where only a few (cut) nuclei remained, after which image acquisition started with the lowest slice. Voxel size at the specimen level was $0.49 \times 0.49 \times 0.49$ μm^3 for the $\times$40 objective, and $0.29 \times 0.29 \times 0.29$ μm^3 for the $\times$100 objective (NB: resolution in z-direction is lower than in x–y direction). The dynamic range was 12 bits, in order to accommodate the extended dynamic range of the fluorescence signal. To obtain measurements for at least 300 nuclei as previously set [12], 12 fields of vision were imaged for each magnification. The fields of vision were approximately 2 mm apart to avoid any bleaching of neighboring fields during image acquisition. Analysis was stopped when sufficient nuclei were collected. Hence, usually some of the image stacks were not analyzed for the $\times$60 magnification. Results of independent experiments were combined by quadratic averag-

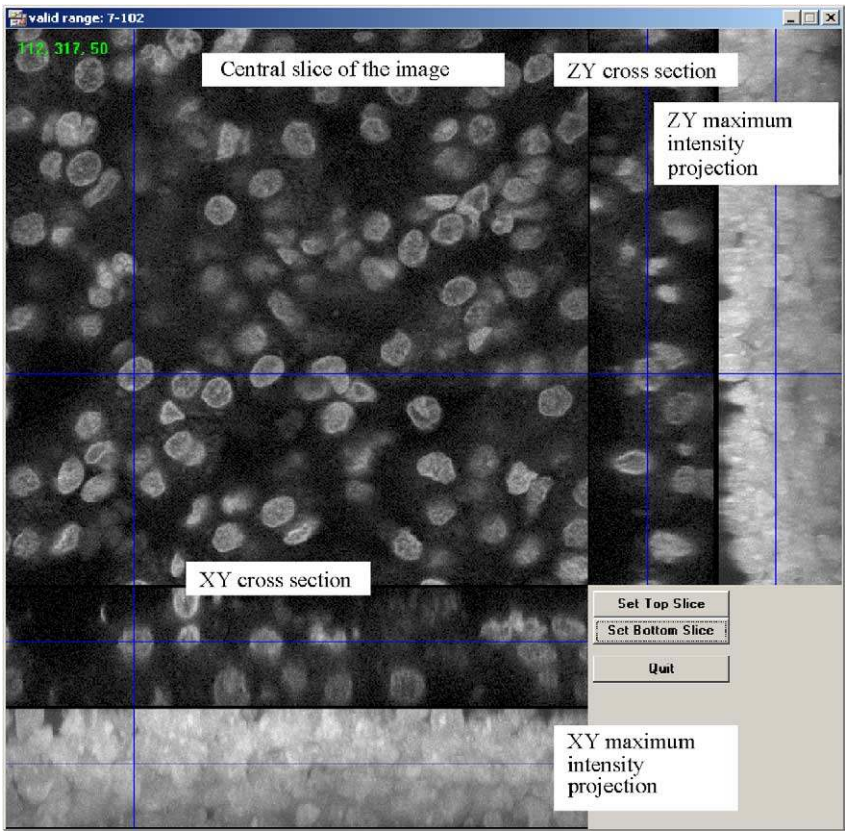

Fig. 1. ZX and YZ projections and cross sections obtained with 3D DNA confocal laser scanning based image cytometry of adrenal tissue, allowing to identify and remove nuclei that have been cut-off at the top or the bottom of the 14 μm thick section. The crosshair defines the planes that are being shown at the right and the bottom sides, while the maximum intensity projections are obtained from the entire image stack and do not change with the position of the crosshair.

ing. The differences between the individual CVs were small indicating high reproducibility.

The image stacks were analyzed off-line using in-house developed software [2]. A complete description of this software is beyond the scope of this paper, but we will describe the most important characteristics here. Segmentation of the nuclei started from the central slice towards both the top and the bottom of the stack. For each slice the nuclei were segmented from the background based on a global threshold value. The nuclei found in the binary image were labeled and indentations were located to split neighboring objects. All background pixels enclosed within object boundaries were added to the surrounding nucleus to avoid nuclei with holes. Next, correctly segmented nuclei were automatically selected based on the total volume of a nucleus, the number of slices encompassed by a nucleus, the longest axis of a set of fitted ellipses for each slice and the roundness defined as both the average and the standard deviation of all contour ratios. The contour ratio itself is computed as the square root of the ratio of the squared perimeter and 4π times the area. Thresholds for this were set by comparing these features between valid segmented nuclei and interactively identified artifacts in a set of 617 objects. To avoid cut-off nuclei the top and bottom of the stacks were identified from ZX and YZ projections (Fig. 1). From these projections nuclei that were either physically cut at the microtome or optically cut by the microscope were without difficulty identified. By selecting lower and upper boundaries these nuclei were automatically excluded from analysis. All grey values within the segmentation mask were integrated to yield a measure for the DNA content of each individual nucleus. The DNA content of all individual nuclei was depicted in DNA histograms. The CV of the diploid peak in each histogram was obtained with the MultiCycle software program (Phoenix Flow Systems, San Diego, CA) as described before [3]. The histograms were standardized to have 50 bins and scaled to 10c

because the number of bins theoretically influences the fitting procedure. It finds the best fit of several curves through the data points, including the Gaussian G0/1 and G2/M phase components. The CV is based upon this mathematical model of the DNA content distribution. Linearity of the system was also assessed with MultiCycle by calculating the G2/G1 ratios.

3. Results

The system for automated segmentation was able to segment approximately 60% of the nuclei correctly without the need for any user interaction. During manual intervention about 5–10% of the rejected nuclei were found to be lymphocytes. The other fraction contained nuclei that were positioned either on top of each other or next to each other.

Table 1 shows that in the first experiment, the best CVs were achieved with TO-PRO-3 staining of adrenal tissue. Table 2 lists the results for the experiment where the optimal duration of application of RNase was determined for adrenal tissue stained with TO-PRO-3. The CVs between RNase incubation for 1 or 18 hours did not vary much, but the CV for the experiment when no RNase was applied was lowest. In Table 3, the influence of pre-treatment is listed for 2 different magnifications. Pre-treatment with cooking in citrate buffer or hydrolysis deteriorated the CVs when RNase was applied for 1 hour and staining was done with TO-PRO-3. Imaging at $\times 60$ instead of $\times 100$ appeared not to deteriorate the CVs for the 2 best protocols.

In Fig. 2, the DNA histogram obtained after analysis with the MultiCycle program is given. This histogram was obtained with the optimal staining protocol (adrenal tissue, no pretreatment, RNase for 1 hour, imaging at $\times 100$ magnification). The 2c peak

Table 1

Comparison of coefficients of variations (CVs) of DNA histograms obtained with confocal laser scanning microscopy based 3D DNA cytometry using 2 tissue types and 2 DNA binding dyes

	CV (%)	
	Liver $\times 100$	Adrenal $\times 100$
YOYO-1	18.0	16.3
TO-PRO-3	16.1	11.6

Table 2

Comparison of coefficients of variations (CVs) of DNA histograms obtained with confocal laser scanning microscopy based 3D DNA cytometry in normal adrenal tissue stained with TO-PRO-3 iodide and treated with RNase for 0, 1 or 18 hours

Duration of RNase treatment (hr)	CV (%)
0	13.8
1	10.3
18	11.4

Table 3

Comparison of coefficients of variations (CVs) of DNA histograms obtained with confocal laser scanning microscopy based 3D DNA cytometry (at $\times 60$ or $\times 100$ final magnifications) in normal adrenal tissue stained with TO-PRO-3 iodide and undergoing different pre-treatment steps. After the pre-treatment procedure, RNase was applied for 1 hour

	CV $\times 60$ (%)	CV $\times 100$ (%)
No pre-treatment	11.4	10.3
Boiling with citrate for 10 mins	15.9	13.5
Hydrolysis 2N HCl	18.2	n/a

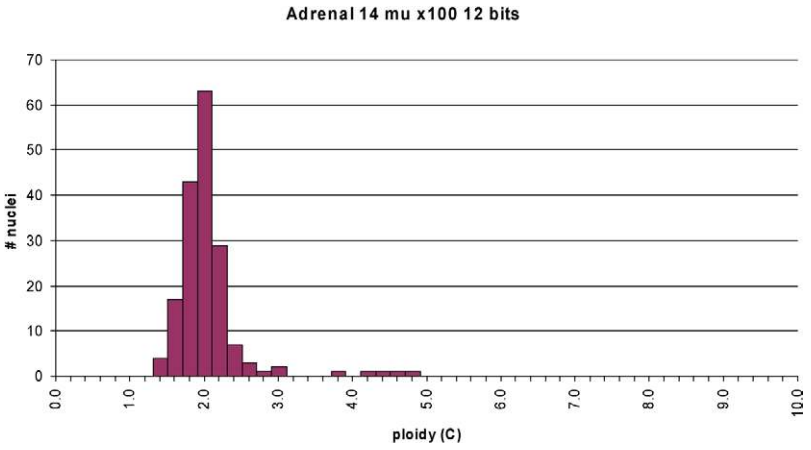

Fig. 2. Example of DNA histogram obtained by 3D DNA confocal laser scanning based image cytometry of 14 μm thick section of adrenal tissue, stained with TO-PRO-3 after 1 hour RNase application and imaging at $\times 100$.

was well-defined and a few nuclei in the G2/M phase were identified. The system appeared to be reasonably linear with a G2/G1 ratio of 2.07.

4. Discussion

The aim of this study was to describe the conditions for accurate and fast 3D CLSM cytometry with a minimum of user interaction. To this end, previously described in-house software [2] was further developed to improve the throughput of the existing software and to ensure that all nuclei were measured unimpaired. After interactively setting the top and bottom slice of the field of vision based on the ZX and YZ projections, image recording and segmentation of nuclei was done automatically. Next, artifacts were automatically removed based on volume, number of slices, size and roundness. Afterwards, only a minimum amount of inspection and correction of segmented objects by the user was necessary. All together, completing a measurement took approximately 3 hours, divided over acquisition, processing and manual intervention as follows: 45 minutes acquisition, 15 minutes automated segmentation and 2 hours of manual intervention. Although this still is relatively long, this new approach does allow pilot clinical studies with this advanced technology for the first time. As operator variability is minimized, sampling can be performed unbiased and reproducibility is probably at its highest. To further increase the sample size and reduce operator bias we are developing a system for automated systematic random sampling of fields of vision. Further progress to reduce the time of analysis will largely depend on improvements in the speed of image acquisition with the CLSM and improvements of Z-resolution that will make segmentation easier. Finally, a reduction of the number of slices will also make results available in a shorter period of time, but this may lead to less accurate results. Furthermore, semi-cubic voxels (the 3D equivalent of a pixel) are more suitable for texture analysis.

We analyzed different tissue processing and imaging variables in normal liver and adrenal tissue. Liver was chosen because it is known that the presence of 4N nuclei is relatively high and it has ample cytoplasm facilitating nuclear segmentation and assessment of linearity. Adrenal tissue was selected as an alternative with expected similar features. Adrenal tissue appeared to provide better CVs, but it is unclear why. DNA cytometry showed comparable results (results not shown), so apparently adrenal tissue is less sensitive to tissue processing than normal liver.

TO-PRO-3, a relatively new stoichiometric DNA binding fluorescent dye [15], provided consistently better CVs than YOYO-1. This can be explained by the fact that TO-PRO-3 is a smaller molecule that better penetrates the 14 μm thick sections and thereby provides a more homogeneous staining throughout the section than YOYO-1. This was indeed visually confirmed. The lower intensity of the fluorescent signal from TO-PRO-3 compared to YOYO-1 appeared not to be a disadvantage; segmentation from the background was still relatively easy. With TO-PRO-3, a clear improvement in the uniformity and reproducibility of quantitative DNA staining in routinely processed formalin fixed tissue was obtained.

RNase incubation was applied to make sure that no RNA remained, although affinity of TO-PRO-3 for RNA is low [4]. Incubation for more than 1 hour did not clearly influence the results, so for practical reasons this incubation period is to be preferred. Antigen retrieval was tested as this has proven to lead to better results for DNA flow cytometry of paraffin embedded tissue [9]. Cooking in citrate buffer and hydrolysis, however, deteriorated the CVs for 3D confocal DNA cytometry. A possible explanation for this is that the nuclear membrane bursts open and DNA flows out of the nucleus.

After having used the $\times 100$ magnification as a gold standard, we tested also a $\times 60$ magnification as this increases throughput, especially during acquisition (the desired number of nuclei are expected to be imaged with 5 stacks instead of 12) but also during manual intervention (a typical nucleus will encompass fewer slices). Fortunately, imaging at $\times 60$ did not deteriorate CVs, indicating that 3D DNA ploidy measurements can well be done at this magnification.

Besides tissue preparation, factors that may influence the CV include laser stability, performance of the photo multiplier, system linearity, dynamic range, Z-resolution, and lens quality. Each of these factors should be optimized for best performance. It is expected that with each new generation of CLSM, some of these system variables will be improved. Especially increasing Z-resolution with a novel technique like 4Pi microscopy [8] is promising in this respect.

5. Conclusion

In conclusion, we developed a protocol for accurate measurement of DNA content in thick histological sec-

tions using CLSM. We showed that the proposed technique allows tissue processing to obtain a largely unbiased sample of nuclei for reproducible 3D DNA cytometry within a time frame acceptable for pilot clinical applications. Further studies will reveal whether this approach yields clinically or biologically useful data.

References

[1] J. Adolfsson, Prognostic value of deoxyribonucleic acid content in prostate cancer: a review of current results, *Int. J. Cancer* **58** (1994), 211.

[2] J.A. Belien, A.H. van Ginkel, P. Tekola, L.S. Ploeger, N.M. Poulin, J.P. Baak and P.J. van Diest, Confocal DNA cytometry: a contour-based segmentation algorithm for automated three-dimensional image segmentation, *Cytometry* **49** (2002), 12.

[3] E. Bergers, P.J. van Diest and J.P. Baak, Reliable DNA histogram interpretation. Number of nuclei requiring measurement with flow cytometry, *Anal. Quant. Cytol. Histol.* **19** (1997), 277.

[4] K. Bink, A. Walch, A. Feuchtinger, H. Eisenmann, P. Hutzler, H. Hofler and M. Werner, TO-PRO-3 is an optimal fluorescent dye for nuclear counterstaining in dual-colour FISH on paraffin sections, *Histochemistry and Cell Biology* **115** (2001), 293.

[5] A. Bocking, J. Stockhause and D. Meyer-Ebrecht, Towards a single cell cancer diagnosis. Multimodal and monocellular measurements of markers and morphology (5M), *Cell. Oncol.* **26** (2004), 73.

[6] C. Boudry, P. Herlin, M. Coster and J.L. Chermant, Influence of sample size on image cytometry of DNA ploidy measurements, *Anal. Quant. Cytol. Histol.* **21** (1999), 209.

[7] R. Chamgoulov, P. Lane and C. Macaulay, Optical computed-tomographic microscope for three-dimensional quantitative histology, *Cell. Oncol.* **26** (2005), 319.

[8] S.W. Hell, M. Schrader and H.T. van der Voort, Far-field fluorescence microscopy with three-dimensional resolution in the 100-nm range, *J. Microsc.* **187** (1997), 1.

[9] M.P. Leers, B. Schutte, P.H. Theunissen, F.C. Ramaekers and M. Nap, Heat pretreatment increases resolution in DNA flow cytometry of paraffin-embedded tumor tissue, *Cytometry* **35** (1999), 260.

[10] T. Mattfeldt, D. Trijic, H. Gottfried and H.A. Kestler, Classification of incidental carcinoma of the prostate using learning vector quantization and support vector machines, *Cell. Oncol.* **26** (2004), 45.

[11] A. Panizo-Santos, J.J. Sola, F.J. Pardo-Mindan, M. Hernandez, E. Cenarruzabeitia and J. Diez, Angiotensin converting enzyme inhibition prevents polyploidization of cardiomyocytes in spontaneously hypertensive rats with left ventricular hypertrophy, *J. Pathol.* **177** (1995), 431.

[12] L.S. Ploeger, J.A. Belien, N.M. Poulin, W. Grizzle and P.J. van Diest, Confocal 3D DNA cytometry: assessment of required coefficient of variation by computer simulation, *Cell. Oncol.* **26** (2004), 93.

[13] J.P. Rigaut, J. Vassy, P. Herlin, F. Duigou, E. Masson, D. Briane, J. Foucrier, S. Carvajal-Gonzalez, A.M. Downs and A.M. Mandard, 3-dimensional DNA image cytometry by confocal scanning laser microscopy in thick tissue blocks, *Cytometry* **12** (1991), 511.

[14] Z. Sapi, J.B. Hendricks, P.G. Pharis and E.J. Wilkinson, Tissue section image analysis of breast neoplasms. Evidence of false aneuploidy, *Am. J. Clin. Pathol.* **99** (1993), 714.

[15] K.M. Sovenyhazy, J.A. Bordelon and J.T. Petty, Spectroscopic studies of the multiple binding modes of a trimethine-bridged cyanine dye with DNA, *Nucleic Acids Res.* **31** (2003), 2561.